

Cite as: K. Ito *et al.*, *Science*
10.1126/science.aaf5530 (2016).

Self-renewal of a purified *Tie2*⁺ hematopoietic stem cell population relies on mitochondrial clearance

Kyoko Ito,^{1,2,3} Raphaël Turcotte,⁴ Jinhua Cui,^{1,5*} Samuel E. Zimmerman,^{1,6*} Sandra Pinho,^{1,5*} Toshihide Mizoguchi,^{1,5} Fumio Arai,⁷ Judith M. Runnels,⁴ Clemens Alt,⁴ Julie Teruya-Feldstein,⁸ Jessica C. Mar,^{1,6,9} Rajat Singh,^{2,10,11} Toshio Suda,^{7,12} Charles P. Lin,⁴ Paul S. Frenette,^{1,2,3,5} Keisuke Ito^{1,2,3,5,11†}

¹Ruth L. and David S. Gottesman Institute for Stem Cell and Regenerative Medicine Research, Albert Einstein College of Medicine, Bronx, NY, USA. ²Department of Medicine, Albert Einstein College of Medicine, Bronx, NY, USA. ³Albert Einstein Cancer Center, Albert Einstein College of Medicine, Bronx, NY, USA. ⁴Center for Systems Biology, Advanced Microscopy Program, Wellman Center for Photomedicine, Massachusetts General Hospital, Harvard Medical School, Boston, MA, USA. ⁵Departments of Cell Biology and Stem Cell Institute, Albert Einstein College of Medicine, Bronx, NY, USA. ⁶Department of Systems and Computational Biology, Albert Einstein College of Medicine, Bronx, NY, USA. ⁷Department of Cell Differentiation, The Sakaguchi Laboratory of Developmental Biology, School of Medicine, Keio University, Japan. ⁸Department of Pathology, Sloan-Kettering Institute, Memorial Sloan-Kettering Cancer Center, New York, NY, USA. ⁹Department of Epidemiology and Population Health, Albert Einstein College of Medicine, Bronx, NY, USA. ¹⁰Department of Molecular Pharmacology, Albert Einstein College of Medicine, Bronx, NY, USA. ¹¹Diabetes Research Center, Albert Einstein College of Medicine, Bronx, NY, USA. ¹²Cancer Science Institute of Singapore, National University of Singapore, Singapore.

*These authors contributed equally to this work.

†Corresponding author. Email: keisuke.ito@einstein.yu.edu

A single hematopoietic stem cell (HSC) is capable of reconstituting hematopoiesis and maintaining homeostasis by balancing self-renewal and cell differentiation. The mechanisms of HSC division balance, however, are not yet defined. Here we demonstrate, by characterizing at the single cell level a purified and minimally heterogeneous *Tie2*⁺ HSC population, that these top hierarchical HSCs preferentially undergo symmetric divisions. The induction of mitophagy, a quality-control process in mitochondria, plays an essential role in self-renewing expansion of *Tie2*⁺ HSCs. Activation of PPAR-fatty acid oxidation promotes to expand *Tie2*⁺ HSCs through enhanced Parkin recruitment in mitochondria. These metabolic pathways are conserved in human *TIE2*⁺ HSCs. Our data thus identify mitophagy as a key mechanisms of HSC expansion, and suggest potential methods of cell fate manipulation through metabolic pathways.

Precise mechanisms enable efficient and regulated HSC renewal versus differentiation, and these processes are coordinated. HSCs must withstand various stresses to maintain life-long hematopoiesis. The repair or clearance of damage is critical to precisely controlling their cell fates and maintaining stemness upon division, especially during HSC expansion through symmetric self-renewing division. HSC exhaustion can result from defective cellular metabolism and/or impaired autophagy (1–6), a lysosomal degradation pathway that degrades damaged or unwanted proteins/organelles (7). The Forkhead Box O3a (FOXO3A)-driven pro-autophagy program, for example, protects HSCs from metabolic stress (5). In a similar process in mammary epithelial stem-like cells, older mitochondria are pushed into daughter cells which are fated to cell differentiation by asymmetric division, thus maintaining high-quality stem cell homeostasis (8). Despite extensive study of HSC renewal and differentiation, however, much remains unclear regarding the mechanisms of division balance due to the heterogeneity of HSC-enriched fractions.

In searching for a potential HSC marker, we observed high *Tie2* levels in the CD34⁺ HSC-enriched compartment (fig. S1A). We therefore established a *Tie2*-GFP reporter line

(*Tie2*-reporter mice or *Tie2* Tg) to validate *Tie2*-expression as a HSC marker (fig. S1, B and C). *Tie2*-GFP was specifically enriched in the HSC fraction but was reduced during differentiation in parallel with mRNA levels (fig. S1, D to G). *Tie2*-GFP positive and negative fractions in CD34⁺CD150⁺CD48^{low}-CD135-KSL cells were purified from *Tie2* reporter mice (hereafter, *Tie2*-GFP^{pos} or *Tie2*-GFP^{neg} HSCs), and *Tie2* levels were detected in *Tie2*-GFP^{pos} but not in *Tie2*-GFP^{neg} HSCs (fig. S1H). The cell cycle kinetics (9) revealed that cell cycling was slightly slower in *Tie2*-GFP^{pos} than in *Tie2*-GFP^{neg} HSCs (fig. S1I). A higher proportion of phenotypic *Tie2*-GFP^{pos} HSCs than *Tie2*-GFP^{neg} HSCs were closely associated with arteriolar structure (fig. S1J), and expressed endothelial and HSC markers (10, 11) (fig. S1, K to M).

In addition, the *Tie2*-GFP^{pos} fraction displayed a highly significant (5.75-fold) increase in LTC-IC frequency relative to the *Tie2*-GFP^{neg} fraction (Fig. 1A). Single cell transplantation showed that a high percentage of single *Tie2*-GFP^{pos} cells (68.0%) exhibited reconstitution capacity without lineage bias and maintained high donor-chimerism upon secondary transplantation. Donor contribution was observed in all recipients transplanted with three *Tie2*-GFP^{pos} HSCs, whereas 40% showed reconstitution capacity with three

Tie2-GFP^{neg} HSCs (Fig. 1B and fig. S2, A to D), demonstrating that *Tie2*-GFP identifies a HSC fraction with minimal heterogeneity. To deliver individual HSCs into bone marrow with certainty, single *Tie2*-GFP^{pos} HSCs were delivered near an opening to the marrow of live mice under multiphoton microscopy guidance (local transplantation, fig. S2E), and tracked during their subsequent homing to locations some distance from the delivery site (Fig. 1C and movies S1 and S2). Recipients showed reconstitution from locally-transplanted single (100%) and multiple *Tie2*-GFP^{pos} HSCs (fig. S2F). A single *Tie2*-GFP^{pos} HSC can exhibit reconstitution capacity in recipient mouse for over 6 months, once it is located in bone marrow.

We also tested, *in vivo* and *in vitro*, whether *Tie2* acts as an HSC marker under stress conditions. 65.0% of polyinosinic:polycytidylic acid (pIpC, inducing the interferon response)-treated single *Tie2*-GFP^{pos} HSCs showed repopulation capacity at levels comparable to control mice (fig. S3, A to D). But while the *Tie2*-GFP^{pos}/*Tie2*-Ab^{pos} fraction exhibited high reconstitution capacity, neither the *Tie2*-GFP^{neg}/*Tie2*-Ab^{pos} fraction nor any of the 12 single *Tie2*-GFP^{pos} KSL cells showed high reconstitution. The majority of the re-sorted *Tie2*-GFP^{pos} cells (70.6% after 3 day culture; 85.7% after 7 day) exhibited multi-lineage reconstitution, though *Tie2*-GFP^{neg} cells did not. None of 90 *Tie2*-GFP^{neg} HSCs provided donor-derived *Tie2*-GFP^{pos} HSCs in recipient mice. These data suggest that *Tie2* serves as a useful marker that can prospectively identify HSCs (figs. S2G and S3, E to L).

Single-cell gene expression assays showed that a substantial number of genes, including HSC factors/markers (e.g., *Tie2*, *Hif1a*, *Mpl* and *Foxo3a*), as well as *Promyelocytic leukemia* (*Pml*) and its downstream signaling pathways, which regulate fatty acid oxidation (FAO) via *Cpt1a* (*Carnitine Palmitoyltransferase 1a*), *Ppard* (*Peroxisome proliferator-activated receptor-delta*) and *Acox1* (*Acyl-CoA Oxidase1*), were markedly higher in the *Tie2*-GFP^{pos} than the *Tie2*-GFP^{neg} fraction (Fig. 1D). Hierarchical clustering, HSC signature, and signatures for both PPAR signaling and fatty acid metabolism demonstrate that *Tie2*-GFP^{pos} HSCs are molecularly farther away from both KSL cells and *Tie2*-GFP^{neg} HSCs (fig. S4). PPAR-FAO's roles in *Tie2*-GFP^{pos} HSCs were then assessed. Impaired reconstitution ability of single *Pml*^{-/-} *Tie2*-GFP^{pos} HSCs could be rescued by GW501516, a PPAR δ -specific agonist (fig. S5, A to C). Thus the PPAR-FAO pathway plays critical roles in directly regulating the self-renewal of the top hierarchical HSCs.

Mitochondria are central metabolic organelles responsible for the final steps of FAO, which cleaves two carbons every cycle to form acetyl-CoA once activated fatty acids have been imported into the mitochondrial matrix (12). Our gene expression assays revealed higher expression of mitochondrial autophagy (mitophagy)-related genes, including

Parkin (*Park2*), *Pink1* (*PTEN-induced putative kinase 1*), *Optineurin*, *Tom 7*, *Map1lc3a* (*Lc3*) and *p62/Sqstm1* in *Tie2*-GFP^{pos} HSCs at steady state. Most of these genes were further upregulated by PPAR-FAO activation (Fig. 2A and fig. S5, D to F). To assess whether mitophagy-related genes are regulated by the PPAR-FAO pathway at the transcriptional level, *Pink1*-luciferase reporters were utilized. PPAR δ agonist transactivated *Pink1* reporters, which were reduced by FAO inhibition or mutation of FOXO-response elements (FRE). *Foxo3a* was upregulated in HSCs upon treatment with PPAR δ agonist, and this was attenuated by the ablation of *Ppard* or *Cpt2*, a FAO-related gene. These data suggested that the PPAR-FAO pathway transcriptionally regulates PINK1 in part through FOXO3a (fig. S6).

We then sought to determine whether PPAR δ -induced mitophagy correlates with a specific metabolic state or profile. Cellular FAO activity was specifically enhanced after PPAR δ -agonist treatment and was accompanied by *Pink1* protein, whereas glucose uptake or levels of pyruvate and TCA cycle metabolites was not altered (fig. S7, A to D). PPAR δ agonists also enhanced mitophagy, with the increased co-localization of Tom20 (Translocase of outer membrane 20) with LAMP1 (Lysosomal-associated membrane protein 1). Flux analyses were then performed to quantify mitochondrial turnover in lysosomes (the organelles where mitophagy occurs) by evaluating the accumulation of Tom20 in the presence of leupeptin, an inhibitor of lysosomal proteolysis. Pharmacological PPAR-FAO activation enhanced the net mitochondrial flux toward lysosomal degradation. These data strongly suggest that PPAR-FAO activates mitophagy (Fig. 2, B and C).

Other findings supported the enhancement of mitophagy by PPAR agonist, including increased co-localization of Parkin with pyruvate dehydrogenase (PDH), a matrix mitochondrial protein. Mitophagy enhancement was again confirmed in GW501516-treated HSCs by the increased co-localization of Parkin with both Tom20 and the autophagosome marker LC3 (figs. S7E and S8, A to D). To explore another mitophagy indicator, mitochondrial DNA (mtDNA) nucleoids were quantified after mitochondrial damage with oligomycin/antimycin A. GW501516-treated HSCs were nearly devoid of mtDNA, and exhibited increased net mtDNA flux, whereas mtDNA was still partially retained in control HSCs (Fig. 2D). Thus damaged mitochondria are cleared more quickly due to enhanced mitophagy activation in *Tie2*-GFP^{pos} HSCs treated with PPAR agonist.

Hematopoiesis-specific *Ppard* conditional knockout mice were then generated. *Ppard*-deleted HSCs exhibited neither enhanced Tom20/Parkin co-localization nor increased mitochondrial net flux after PPAR δ agonist treatment, although these agonists stimulated mitophagy in wild-type HSCs, and a mitochondrial uncoupler, carbonyl cyanide *m-*

chlorophenylhydrazine (CCCP), induced mitophagy in both genotyped HSCs (fig. S8E). Conditional heterozygous deletion of *Cpt2* partially but significantly attenuated the enhanced Parkin recruitment in mitochondria induced by PPAR agonist (fig. S8F). Taken together, these direct genetic approaches reveal that PPAR δ agonists stimulate mitophagy in a PPAR-FAO-dependent manner.

To test whether mitophagy is critical for *Tie2*-GFP^{pos} HSC expansion, *Parkin* and *Pink1* were first silenced by RNA interference (RNAi)-mediated knockdown. siPark2 decreased net mitochondrial flux (a hallmark of mitophagy) in GW501516-treated HSCs as indicated by decreased co-localization of Tom20 and PDH with LAMP1, whereas cell death, proliferation rate, FAO activity, and *Cdk6* levels was not altered (Fig. 3A and figs. S7A and S9). *Parkin*-knockdown in GW501516-treated HSCs led to accumulating signals of Tom20 and PDH, and reduced co-localization of LAMP1 with LC3 (fig. S10, A to C). mtDNA was retained in *Parkin*-silenced HSCs, and these cells were refractory to PPAR agonist (Fig. 3B and fig. S10D). These data suggest that Parkin has an essential role in PPAR-FAO-induced mitophagy.

Since *Pink1* is known to be essential for mitophagy and *Pink1* levels were increased by PPAR-FAO activation, we then assessed the effect of knock-down of *Pink1* on the process. *Pink1*-silencing reduced Tom20 co-localization with both LAMP1 and Parkin, and net flux of mitochondria in GW501516-treated HSCs, accompanied by accumulating Tom20 signals. mtDNA was also retained in *Pink1*-silenced HSCs (Fig. 3, B and C, and fig. S10, D to G). Consequently, Parkin and *Pink1* play important roles in PPAR-FAO-induced mitophagy in HSCs.

Potential clinical applications of pharmacological FAO modulation in human hematopoiesis were then explored. *TIE2* expression is enriched in the HSC fraction, and *TIE2*-positivity enhances LTC-IC frequency and in vivo repopulation capacity in human bone marrow (fig. S11, A to G). GW501516 enhances LTC-IC frequency with mitophagy activation, whereas low doses of FAO inhibitor reduce its capacity. Fatty acid metabolism therefore can control self-renewal capacity and the cell fates of human HSCs (Fig. 3D and fig. S11, H to J).

Finally, we explored the effects of FAO-induced mitophagy on *Tie2*-GFP^{pos} HSC expansion. In vivo paired daughter cell (PDC) assays can determine the division patterns of HSCs retrospectively, by assessing the reconstitution capacity of each daughter cell (3, 13). In vivo PDC assays revealed that *Tie2*-GFP^{pos} HSCs preferentially undergo SD (symmetric division) (in 20 out of 27 divisions, or 74.1%, both daughter cells showed a reconstitution capacity), rather than AD (asymmetric division) or SC (symmetric commitment, both daughter cells exhibited no reconstitution capacity), where-

as *Tie2*-GFP^{neg} HSCs undergo either AD or SC (Fig. 4, A to C, and fig. S12). To further test the restoration capacity of hematopoiesis by single *Tie2*-GFP^{pos} HSCs, we performed transplantation assays under high stress conditions, as are found in single-cell transplantation without supporting cells. The survival ratio after single *Tie2*-GFP^{pos} HSC transplantation was 85.7%, whereas no recipients of single *Tie2*-GFP^{neg} HSCs survived (Fig. 4D and fig. S13, A and B). There are functional HSCs in the *Tie2*-GFP^{neg} fraction, but they fail to adequately respond to the demand for hematopoietic recovery under high stress conditions without the enhanced symmetric expansion provided by *Tie2*-GFP^{pos} HSCs.

As expected, PPAR-FAO increased the number of *Tie2*-GFP^{pos} cells in vitro with an increased rate of SD (fig. S13, C to G). *Tie2*-GFP^{pos} HSC numbers were increased compared to the original number of transplanted donor cells in recipients, and was further increased by PPAR δ agonist (~4 times). Furthermore, PPAR δ agonist expanded *Tie2*-GFP^{pos} HSCs under physiological stress as induced by pIpC (Fig. 4E and figs. S2Eii and S13H).

However, silencing *Park2* or *Pink1* not only abrogated the expansion of *Tie2*-GFP^{pos} cells in vitro, but also inhibited their maintenance (fig. S13I). Most single *Parkin*-silenced *Tie2*-GFP^{pos} cells failed to show reconstitution capacity (92.3%), whereas the majority of control *Tie2*-GFP^{pos} cells (66.7%) exhibited reconstitution capacity (Fig. 4F and fig. S13J). *Pink1*^{-/-} HSC failed to adequately respond to the demand for hematopoietic recovery under high stress conditions even though PPAR δ agonist was administered (fig. S13K). In conclusion, *Tie2*-GFP^{pos} HSCs can maintain stem cell potential during cell cycling due to high mitochondrial clearance through mitophagy and upregulation of *Parkin* and *Pink1* (fig. S14). Our data from this highly purified HSC fraction identifies mitochondrial clearance by induction of mitophagosome formation as a key mechanism in maintaining stemness.

REFERENCES AND NOTES

1. K. Ito, T. Suda, Metabolic requirements for the maintenance of self-renewing stem cells. *Nat. Rev. Mol. Cell Biol.* **15**, 243–256 (2014). [doi:10.1038/nrm3772](https://doi.org/10.1038/nrm3772) [Medline](#)
2. N. Shyh-Chang, G. Q. Daley, L. C. Cantley, Stem cell metabolism in tissue development and aging. *Development* **140**, 2535–2547 (2013). [doi:10.1242/dev.091777](https://doi.org/10.1242/dev.091777) [Medline](#)
3. K. Ito, A. Carracedo, D. Weiss, F. Arai, U. Ala, D. E. Avigan, Z. T. Schafer, R. M. Evans, T. Suda, C.-H. Lee, P. P. Pandolfi, A PML-PPAR- δ pathway for fatty acid oxidation regulates hematopoietic stem cell maintenance. *Nat. Med.* **18**, 1350–1358 (2012). [doi:10.1038/nm.2882](https://doi.org/10.1038/nm.2882) [Medline](#)
4. M. Mohrin, J. Shin, Y. Liu, K. Brown, H. Luo, Y. Xi, C. M. Haynes, D. Chen, A mitochondrial UPR-mediated metabolic checkpoint regulates hematopoietic stem cell aging. *Science* **347**, 1374–1377 (2015). [doi:10.1126/science.1263611](https://doi.org/10.1126/science.1263611) [Medline](#)
5. M. R. Warr, M. Binnewies, J. Flach, D. Reynaud, T. Garg, R. Malhotra, J. Debnath, E. Passegué, FOXO3A directs a protective autophagy program in haematopoietic stem cells. *Nature* **494**, 323–327 (2013). [doi:10.1038/nature11895](https://doi.org/10.1038/nature11895) [Medline](#)
6. M. Mortensen, D. J. P. Ferguson, M. Edelmann, B. Kessler, K. J. Morten, M. Komatsu, A. K. Simon, Loss of autophagy in erythroid cells leads to defective removal of mitochondria and severe anemia in vivo. *Proc. Natl. Acad. Sci. U.S.A.*

- 107, 832–837 (2010) [doi:10.1073/pnas.0913170107](https://doi.org/10.1073/pnas.0913170107) [Medline](#)
7. L. Galluzzi, F. Pietrocola, B. Levine, G. Kroemer, Metabolic control of autophagy. *Cell* **159**, 1263–1276 (2014) [doi:10.1016/j.cell.2014.11.006](https://doi.org/10.1016/j.cell.2014.11.006) [Medline](#)
8. P. Katajisto, J. Döhla, C. L. Chaffer, N. Pentimikko, N. Marjanovic, S. Iqbal, R. Zoncu, W. Chen, R. A. Weinberg, D. M. Sabatini, Asymmetric apportioning of aged mitochondria between daughter cells is required for stemness. *Science* **348**, 340–343 (2015) [doi:10.1126/science.1260384](https://doi.org/10.1126/science.1260384) [Medline](#)
9. F. Arai, A. Hirao, M. Ohmura, H. Sato, S. Matsuoka, K. Takubo, K. Ito, G. Y. Koh, T. Suda, Tie2/angiopoietin-1 signaling regulates hematopoietic stem cell quiescence in the bone marrow niche. *Cell* **118**, 149–161 (2004) [doi:10.1016/j.cell.2004.07.004](https://doi.org/10.1016/j.cell.2004.07.004) [Medline](#)
10. M. Acar, K. S. Kocherlakota, M. M. Murphy, J. G. Peyer, H. Oguro, C. N. Inra, C. Jaiyeola, Z. Zhao, K. Luby-Phelps, S. J. Morrison, Deep imaging of bone marrow shows non-dividing stem cells are mainly perisinusoidal. *Nature* **526**, 126–130 (2015) [doi:10.1038/nature15250](https://doi.org/10.1038/nature15250) [Medline](#)
11. Y. Kunisaki, I. Bruns, C. Scheiermann, J. Ahmed, S. Pinho, D. Zhang, T. Mizoguchi, Q. Wei, D. Lucas, K. Ito, J. C. Mar, A. Bergman, P. S. Frenette, Arteriolar niches maintain haematopoietic stem cell quiescence. *Nature* **502**, 637–643 (2013) [doi:10.1038/nature12612](https://doi.org/10.1038/nature12612) [Medline](#)
12. W. H. Kunau, V. Dommès, H. Schulz, β -oxidation of fatty acids in mitochondria, peroxisomes, and bacteria: A century of continued progress. *Prog. Lipid Res.* **34**, 267–342 (1995) [doi:10.1016/0163-7827\(95\)00011-9](https://doi.org/10.1016/0163-7827(95)00011-9) [Medline](#)
13. R. Yamamoto, Y. Morita, J. Oebara, S. Hamanaka, M. Onodera, K. L. Rudolph, H. Ema, H. Nakauchi, Clonal analysis unveils self-renewing lineage-restricted progenitors generated directly from hematopoietic stem cells. *Cell* **154**, 1112–1126 (2013) [doi:10.1016/j.cell.2013.08.007](https://doi.org/10.1016/j.cell.2013.08.007) [Medline](#)
14. T. Motoike, S. Loughna, E. Perens, B. L. Roman, W. Liao, T. C. Chau, C. D. Richardson, T. Kawate, J. Kuno, B. M. Weinstein, D. Y. R. Stainier, T. N. Sato, Universal GFP reporter for the study of vascular development. *Genesis* **28**, 75–81 (2000) [doi:10.1002/1526-968X\(200010\)28:2<75::AID-GENE50>3.0.CO;2-S](https://doi.org/10.1002/1526-968X(200010)28:2<75::AID-GENE50>3.0.CO;2-S) [Medline](#)
15. Z. G. Wang, L. Delva, M. Gaboli, R. Rivi, M. Giorgio, C. Cordon-Cardo, F. Grosveld, P. P. Pandolfi, Role of PML in cell growth and the retinoic acid pathway. *Science* **279**, 1547–1551 (1998) [doi:10.1126/science.279.5356.1547](https://doi.org/10.1126/science.279.5356.1547) [Medline](#)
16. Y. Barak, D. Liao, W. He, E. S. Ong, M. C. Nelson, J. M. Olefsky, R. Boland, R. M. Evans, Effects of peroxisome proliferator-activated receptor δ on placentation, adiposity, and colorectal cancer. *Proc. Natl. Acad. Sci. U.S.A.* **99**, 303–308 (2002) [doi:10.1073/pnas.012610299](https://doi.org/10.1073/pnas.012610299) [Medline](#)
17. J. Lee, J. M. Ellis, M. J. Wolfgang, Adipose fatty acid oxidation is required for thermogenesis and potentiates oxidative stress-induced inflammation. *Cell Reports* **10**, 266–279 (2015) [doi:10.1016/j.celrep.2014.12.023](https://doi.org/10.1016/j.celrep.2014.12.023) [Medline](#)
18. M. Lazarou, D. A. Sliter, L. A. Kane, S. A. Sarraf, C. Wang, J. L. Burman, D. P. Sideris, A. I. Fogel, R. J. Youle, The ubiquitin kinase PINK1 recruits autophagy receptors to induce mitophagy. *Nature* **524**, 309–314 (2015) [doi:10.1038/nature14893](https://doi.org/10.1038/nature14893) [Medline](#)
19. D. Narendra, A. Tanaka, D.-F. Suen, R. J. Youle, Parkin is recruited selectively to impaired mitochondria and promotes their autophagy. *J. Cell Biol.* **183**, 795–803 (2008) [doi:10.1083/jcb.200809125](https://doi.org/10.1083/jcb.200809125) [Medline](#)
20. D. P. Narendra, S. M. Jin, A. Tanaka, D.-F. Suen, C. A. Gautier, J. Shen, M. R. Cookson, R. J. Youle, PINK1 is selectively stabilized on impaired mitochondria to activate Parkin. *PLoS Biol.* **8**, e1000298 (2010) [doi:10.1371/journal.pbio.1000298](https://doi.org/10.1371/journal.pbio.1000298) [Medline](#)
21. L. A. Scarffe, D. A. Stevens, V. L. Dawson, T. M. Dawson, Parkin and PINK1: Much more than mitophagy. *Trends Neurosci.* **37**, 315–324 (2014). [doi:10.1016/j.tins.2014.03.004](https://doi.org/10.1016/j.tins.2014.03.004) [Medline](#)
22. J. de Boer, A. Williams, G. Skavdis, N. Harker, M. Coles, M. Tolaini, T. Norton, K. Williams, K. Roderick, A. J. Potocnik, D. Kioussis, Transgenic mice with hematopoietic and lymphoid specific expression of Cre. *Eur. J. Immunol.* **33**, 314–325 (2003) [doi:10.1002/immu.200310005](https://doi.org/10.1002/immu.200310005) [Medline](#)
23. D. Walter, A. Lier, A. Geiselhart, F. B. Thalheimer, S. Huntscha, M. C. Sobotta, B. Moehle, D. Brocks, I. Bayindir, P. Kaschutnig, K. Muedder, C. Klein, A. Jauch, T. Schroeder, H. Geiger, T. P. Dick, T. Holland-Letz, P. Schmezer, S. W. Lane, M. A. Rieger, M. A. G. Essers, D. A. Williams, A. Trumpp, M. D. Milsom, Exit from dormancy provokes DNA-damage-induced attrition in haematopoietic stem cells. *Nature* **520**, 549–552 (2015) [doi:10.1038/nature14131](https://doi.org/10.1038/nature14131) [Medline](#)
24. M. A. Essers, S. Offner, W. E. Blanco-Bose, Z. Waibler, U. Kalinke, M. A. Duchosal, A. Trumpp, IFN α activates dormant haematopoietic stem cells in vivo. *Nature* **458**, 904–908 (2009) [doi:10.1038/nature07815](https://doi.org/10.1038/nature07815) [Medline](#)
25. K. Hosokawa, F. Arai, H. Yoshihara, H. Iwasaki, M. Hembree, T. Yin, Y. Nakamura, Y. Gomei, K. Takubo, H. Shiama, S. Matsuoka, L. Li, T. Suda, Cadherin-based adhesion is a potential target for niche manipulation to protect hematopoietic stem cells in adult bone marrow. *Cell Stem Cell* **6**, 194–198 (2010) [doi:10.1016/j.stem.2009.04.013](https://doi.org/10.1016/j.stem.2009.04.013) [Medline](#)
26. M. Hanoun, D. Zhang, T. Mizoguchi, S. Pinho, H. Pierce, Y. Kunisaki, J. Lacombe, S. A. Armstrong, U. Dührsen, P. S. Frenette, Acute myelogenous leukemia-induced sympathetic neuropathy promotes malignancy in an altered hematopoietic stem cell niche. *Cell Stem Cell* **15**, 365–375 (2014) [doi:10.1016/j.stem.2014.06.020](https://doi.org/10.1016/j.stem.2014.06.020) [Medline](#)
27. N. Martinez-Lopez, D. Athanvarangkul, P. Mishall, S. Sahu, R. Singh, Autophagy proteins regulate ERK phosphorylation. *Nat. Commun.* **4**, 2799 (2013) [doi:10.1038/ncomms3799](https://doi.org/10.1038/ncomms3799) [Medline](#)
28. D. J. Klionsky *et al.*, Guidelines for the use and interpretation of assays for monitoring autophagy. *Autophagy* **8**, 445–544 (2012) [doi:10.4161/auto.19496](https://doi.org/10.4161/auto.19496) [Medline](#)
29. L. S. Pike, A. L. Smift, N. J. Croteau, D. A. Ferrick, M. Wu, Inhibition of fatty acid oxidation by etomoxir impairs NADPH production and increases reactive oxygen species resulting in ATP depletion and cell death in human glioblastoma cells. *Biochim. Biophys. Acta* **1807**, 726–734 (2011) [doi:10.1016/j.bbabi.2010.10.022](https://doi.org/10.1016/j.bbabi.2010.10.022) [Medline](#)
30. M. Wu, H. Y. Kwon, F. Rattis, J. Blum, C. Zhao, R. Ashkenazi, T. L. Jackson, N. Gaiano, T. Oliver, T. Reya, Imaging hematopoietic precursor division in real time. *Cell Stem Cell* **1**, 541–554 (2007) [doi:10.1016/j.stem.2007.08.009](https://doi.org/10.1016/j.stem.2007.08.009) [Medline](#)
31. S. J. Song, K. Ito, U. Ala, L. Kats, K. Webster, S. M. Sun, M. Jongen-Lavrencic, K. Manova-Todorova, J. Teruya-Feldstein, D. E. Avigan, R. Delwel, P. P. Pandolfi, The oncogenic microRNA miR-22 targets the TET2 tumor suppressor to promote hematopoietic stem cell self-renewal and transformation. *Cell Stem Cell* **13**, 87–101 (2013) [doi:10.1016/j.stem.2013.06.003](https://doi.org/10.1016/j.stem.2013.06.003) [Medline](#)
32. L. E. Purton, D. T. Scadden, Limiting factors in murine hematopoietic stem cell assays. *Cell Stem Cell* **1**, 263–270 (2007) [doi:10.1016/j.stem.2007.08.016](https://doi.org/10.1016/j.stem.2007.08.016) [Medline](#)
33. J. M. Peters, F. J. Gonzalez, Sorting out the functional role(s) of peroxisome proliferator-activated receptor- β/δ (PPAR β/δ) in cell proliferation and cancer. *Biochim. Biophys. Acta* **1796**, 230–241 (2009). [Medline](#)
34. T. Tanaka, J. Yamamoto, S. Iwasaki, H. Asaba, H. Hamura, Y. Ikeda, M. Watanabe, K. Magoori, R. X. Ioka, K. Tachibana, Y. Watanabe, Y. Uchiyama, K. Sumi, H. Iguchi, S. Ito, T. Doi, T. Hamakubo, M. Naito, J. Auwerx, M. Yanagisawa, T. Kodama, J. Sakai, Activation of peroxisome proliferator-activated receptor δ induces fatty acid β -oxidation in skeletal muscle and attenuates metabolic syndrome. *Proc. Natl. Acad. Sci. U.S.A.* **100**, 15924–15929 (2003) [doi:10.1073/pnas.0306981100](https://doi.org/10.1073/pnas.0306981100) [Medline](#)
35. T. Wurch, D. Junquero, A. Delhon, J. Pauwels, Pharmacological analysis of wild-type α , γ and δ subtypes of the human peroxisome proliferator-activated receptor. *Naunyn Schmiedeberg's Arch. Pharmacol.* **365**, 133–140 (2002) [doi:10.1007/s00210-001-0504-z](https://doi.org/10.1007/s00210-001-0504-z) [Medline](#)
36. B. Dykstra, D. Kent, M. Bowie, L. McCaffrey, M. Hamilton, K. Lyons, S.-J. Lee, R. Brinkman, C. Eaves, Long-term propagation of distinct hematopoietic differentiation programs in vivo. *Cell Stem Cell* **1**, 218–229 (2007) [doi:10.1016/j.stem.2007.05.015](https://doi.org/10.1016/j.stem.2007.05.015) [Medline](#)
37. H. B. Sieburg, R. H. Cho, B. Dykstra, N. Uchida, C. J. Eaves, C. E. Muller-Sieburg, The hematopoietic stem compartment consists of a limited number of discrete stem cell subsets. *Blood* **107**, 2311–2316 (2006) [doi:10.1182/blood-2005-07-2970](https://doi.org/10.1182/blood-2005-07-2970) [Medline](#)
38. Y. Matsuzaki, K. Kinjo, R. C. Mulligan, H. Okano, Unexpectedly efficient homing capacity of purified murine hematopoietic stem cells. *Immunity* **20**, 87–93 (2004) [doi:10.1016/S1074-7613\(03\)00354-6](https://doi.org/10.1016/S1074-7613(03)00354-6) [Medline](#)
39. R. Turcotte, C. Alt, L. J. Mortensen, C. P. Lin, Characterization of multiphoton microscopy in the bone marrow following intravital laser osteotomy. *Biomed. Opt. Express* **5**, 3578–3588 (2014) [doi:10.1364/BOE.5.003578](https://doi.org/10.1364/BOE.5.003578) [Medline](#)
40. D. A. Sipkins, X. Wei, J. W. Wu, J. M. Runnels, D. Côté, T. K. Means, A. D. Luster, D. T. Scadden, C. P. Lin, In vivo imaging of specialized bone marrow endothelial

- microdomains for tumour engraftment. *Nature* **435**, 969–973 (2005).[doi:10.1038/nature03703](https://doi.org/10.1038/nature03703) [Medline](#)
41. C. Lo Celso, H. E. Fleming, J. W. Wu, C. X. Zhao, S. Miake-Lye, J. Fujisaki, D. Côté, D. W. Rowe, C. P. Lin, D. T. Scadden, Live-animal tracking of individual haematopoietic stem/progenitor cells in their niche. *Nature* **457**, 92–96 (2009).[doi:10.1038/nature07434](https://doi.org/10.1038/nature07434) [Medline](#)
 42. C. Lo Celso, C. P. Lin, D. T. Scadden, In vivo imaging of transplanted hematopoietic stem and progenitor cells in mouse calvarium bone marrow. *Nat. Protoc.* **6**, 1–14 (2011).[doi:10.1038/nprot.2010.168](https://doi.org/10.1038/nprot.2010.168) [Medline](#)
 43. J. Schindelin, I. Arganda-Carreras, E. Frise, V. Kaynig, M. Longair, T. Pietzsch, S. Preibisch, C. Rueden, S. Saalfeld, B. Schmid, J.-Y. Tinevez, D. J. White, V. Hartenstein, K. Eliceiri, P. Tomancak, A. Cardona, Fiji: An open-source platform for biological-image analysis. *Nat. Methods* **9**, 676–682 (2012).[doi:10.1038/nmeth.2019](https://doi.org/10.1038/nmeth.2019) [Medline](#)
 44. K. Busch, K. Klapproth, M. Barile, M. Flossdorf, T. Holland-Letz, S. M. Schlenner, M. Reth, T. Höfer, H.-R. Rodewald, Fundamental properties of unperturbed haematopoiesis from stem cells in vivo. *Nature* **518**, 542–546 (2015).[doi:10.1038/nature14242](https://doi.org/10.1038/nature14242) [Medline](#)
 45. R. Gazit, P. K. Mandal, W. Ebina, A. Ben-Zvi, C. Nombela-Arrieta, L. E. Silberstein, D. J. Rossi, *Fgd5* identifies hematopoietic stem cells in the murine bone marrow. *J. Exp. Med.* **211**, 1315–1331 (2014).[doi:10.1084/jem.20130428](https://doi.org/10.1084/jem.20130428) [Medline](#)
 46. A. Sanjuan-Pla, I. C. Macaulay, C. T. Jensen, P. S. Woll, T. C. Luis, A. Mead, S. Moore, C. Carella, S. Matsuoka, T. Bouriez Jones, O. Chowdhury, L. Stenson, M. Lutteropp, J. C. A. Green, R. Facchini, H. Boukarabila, A. Grover, A. Gambardella, S. Thongjuea, J. Carrelha, P. Tarrant, D. Atkinson, S.-A. Clark, C. Nerlov, S. E. W. Jacobsen, Platelet-biased stem cells reside at the apex of the haematopoietic stem-cell hierarchy. *Nature* **502**, 232–236 (2013).[doi:10.1038/nature12495](https://doi.org/10.1038/nature12495) [Medline](#)
 47. M. Osawa, K. Hanada, H. Hamada, H. Nakauchi, Long-term lymphohematopoietic reconstitution by a single CD34-low/negative hematopoietic stem cell. *Science* **273**, 242–245 (1996).[doi:10.1126/science.273.5272.242](https://doi.org/10.1126/science.273.5272.242) [Medline](#)
 48. T. Grinenko, K. Arndt, M. Portz, N. Mende, M. Günther, K. N. Cosgun, D. Alexopoulou, N. Lakshmanaperumal, I. Henry, A. Dahl, C. Waskow, Clonal expansion capacity defines two consecutive developmental stages of long-term hematopoietic stem cells. *J. Exp. Med.* **211**, 209–215 (2014).[doi:10.1084/jem.20131115](https://doi.org/10.1084/jem.20131115) [Medline](#)
 49. J. Flach, S. T. Bakker, M. Mohrin, P. C. Conroy, E. M. Pietras, D. Reynaud, S. Alvarez, M. E. Diolaiti, F. Ugarte, E. C. Forsberg, M. M. Le Beau, B. A. Stohr, J. Méndez, C. G. Morrison, E. Passegué, Replication stress is a potent driver of functional decline in ageing haematopoietic stem cells. *Nature* **512**, 198–202 (2014).[doi:10.1038/nature13619](https://doi.org/10.1038/nature13619) [Medline](#)
 50. A. B. Balazs, A. J. Fabian, C. T. Esmon, R. C. Mulligan, Endothelial protein C receptor (CD201) explicitly identifies hematopoietic stem cells in murine bone marrow. *Blood* **107**, 2317–2321 (2006).[doi:10.1182/blood-2005-06-2249](https://doi.org/10.1182/blood-2005-06-2249) [Medline](#)
 51. H. Oguro, L. Ding, S. J. Morrison, SLAM family markers resolve functionally distinct subpopulations of hematopoietic stem cells and multipotent progenitors. *Cell Stem Cell* **13**, 102–116 (2013).[doi:10.1016/j.stem.2013.05.014](https://doi.org/10.1016/j.stem.2013.05.014) [Medline](#)
 52. J. Y. Chen, M. Miyanishi, S. K. Wang, S. Yamazaki, R. Sinha, K. S. Kao, J. Seita, D. Sahoo, H. Nakauchi, I. L. Weissman, Hoxb5 marks long-term haematopoietic stem cells and reveals a homogenous perivascular niche. *Nature* **530**, 223–227 (2016).[doi:10.1038/nature16943](https://doi.org/10.1038/nature16943) [Medline](#)
 53. A. Wilson, G. M. Oser, M. Jaworski, W. E. Blanco-Bose, E. Laurenti, C. Adolphe, M. A. Essers, H. R. Macdonald, A. Trumpp, Dormant and self-renewing hematopoietic stem cells and their niches. *Ann. N. Y. Acad. Sci.* **1106**, 64–75 (2007).[doi:10.1196/annals.1392.021](https://doi.org/10.1196/annals.1392.021) [Medline](#)
 54. H. Nakauchi, K. Sudo, H. Ema, Quantitative assessment of the stem cell self-renewal capacity. *Ann. N. Y. Acad. Sci.* **938**, 18–25 (2001).[doi:10.1111/j.1749-6632.2001.tb03570.x](https://doi.org/10.1111/j.1749-6632.2001.tb03570.x) [Medline](#)
 55. Y. Mei, Y. Zhang, K. Yamamoto, W. Xie, T. W. Mak, H. You, FOXO3a-dependent regulation of Pink1 (Park6) mediates survival signaling in response to cytokine deprivation. *Proc. Natl. Acad. Sci. U.S.A.* **106**, 5153–5158 (2009).[doi:10.1073/pnas.0901104106](https://doi.org/10.1073/pnas.0901104106) [Medline](#)
 56. T. Suda, J. Suda, M. Ogawa, Disparate differentiation in mouse hemopoietic colonies derived from paired progenitors. *Proc. Natl. Acad. Sci. U.S.A.* **81**, 2520–2524 (1984).[doi:10.1073/pnas.81.8.2520](https://doi.org/10.1073/pnas.81.8.2520) [Medline](#)
 57. S. M. Davidson, T. Papagiannakopoulos, B. A. Olenchock, J. E. Heyman, M. A. Keibler, A. Luengo, M. R. Bauer, A. K. Jha, J. P. O'Brien, K. A. Pierce, D. Y. Gui, L. B. Sullivan, T. M. Wasylenko, L. Subbaraj, C. R. Chin, G. Stephanopoulos, B. T. Mott, T. Jacks, C. B. Clish, M. G. Vander Heiden, Environment impacts the metabolic dependencies of Ras-driven non-small cell lung cancer. *Cell Metab.* **23**, 517–528 (2016).[doi:10.1016/j.cmet.2016.01.007](https://doi.org/10.1016/j.cmet.2016.01.007) [Medline](#)
 58. T. M. Dawson, H. S. Ko, V. L. Dawson, Genetic animal models of Parkinson's disease. *Neuron* **66**, 646–661 (2010).[doi:10.1016/j.neuron.2010.04.034](https://doi.org/10.1016/j.neuron.2010.04.034) [Medline](#)
 59. J. A. Williams, H.-M. Ni, A. Haynes, S. Manley, Y. Li, H. Jaeschke, W.-X. Ding, Chronic deletion and acute knockdown of Parkin have differential responses to acetaminophen-induced mitophagy and liver injury in mice. *J. Biol. Chem.* **290**, 10934–10946 (2015).[doi:10.1074/jbc.M114.602284](https://doi.org/10.1074/jbc.M114.602284) [Medline](#)

ACKNOWLEDGMENTS

We are grateful to all members of the Ito lab and Einstein SCI for their comments on HSC self-renewal, M. Wolfgang, A. Carracedo, H. You, and Flow and Imaging cores (P30CA013330) for help and materials. This work was supported by NIH (R01DK98263 and R01DK100689) and NYSTEM (Single-cell-core, C029154) to K.I., HSCI (to C.P.L.), NIH and Ellison Medical Foundation (to R.S.), NIH and LLS (to P.S.F.), and JSPS (to T.S.). The authors declare no competing financial interests.

SUPPLEMENTARY MATERIALS

www.sciencemag.org/cgi/content/full/science.aaf5530/DC1

Materials and Methods

Supplementary Text

Figs. S1 to S14

References (14–59)

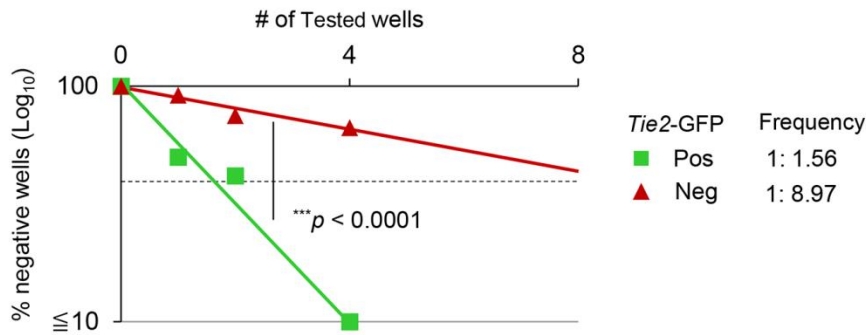
Movies S1 and S2

26 February 2016; accepted 4 October 2016

Published online 13 October 2016

10.1126/science.aaf5530

A LTC-IC in LDA (Limiting-dilution assay)

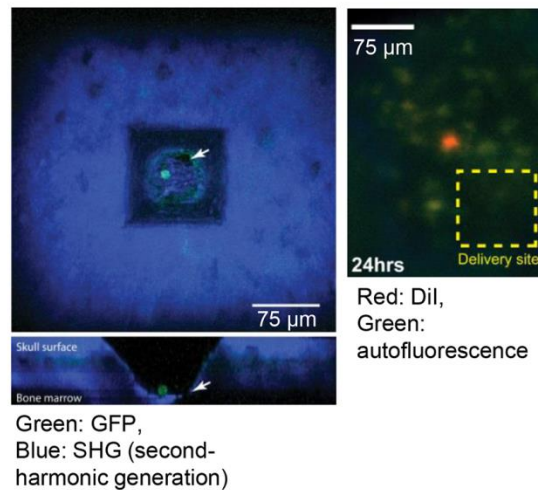


B

Fraction	Cell dose	No. of positive mice
<i>Tie2</i> -GFP ^{pos} HSC	1	34 / 50 (68.0 %)
<i>Tie2</i> -GFP ^{neg} HSC	1	5 / 28 (17.9 %)
<i>Tie2</i> -GFP ^{pos} HSC	3	5 / 5 (100 %)
<i>Tie2</i> -GFP ^{neg} HSC	3	2 / 5 (40.0 %)

HSC : CD34⁺CD150⁺CD48⁻CD135⁻KSL
 Positive reconstitution: over 1% of donor-derived cells

C



D

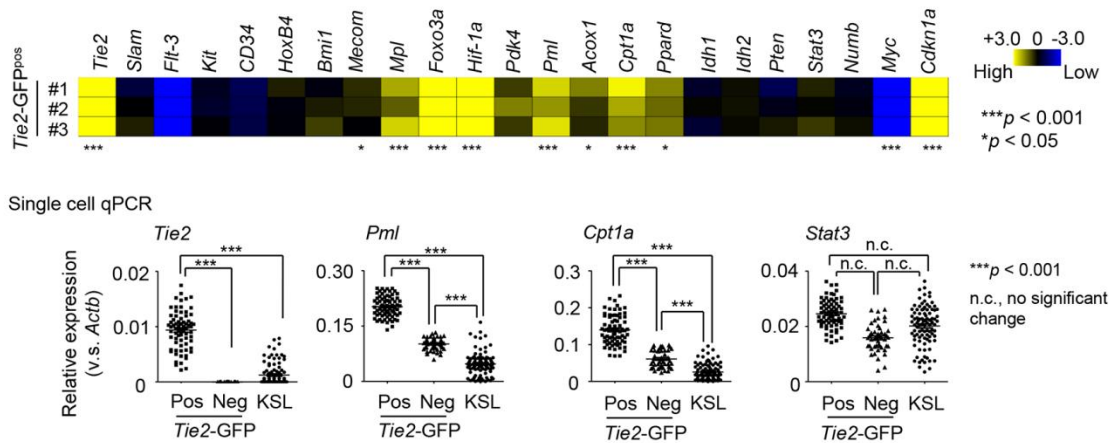


Fig. 1. *Tie2*-GFP marks a distinct HSC subset. (A) LTC-IC frequencies of *Tie2*-GFP^{pos} and *Tie2*-GFP^{neg} HSCs were determined in limiting-dilution assay (LDA). (B) Percentages of successful long-term reconstitution. (C) In vivo imaging of single *Tie2*-GFP^{pos} HSC immediately after local delivery in calvarium. Top (upper) and side (lower) view of delivery site. Arrow, opening to the bone marrow (left). In vivo imaging of the same cell, 24 hours. after local delivery (right, en face maximum intensity projection). (D) Single cell gene expression analysis using BioMark System array (Fluidigm) (also see Methods section).

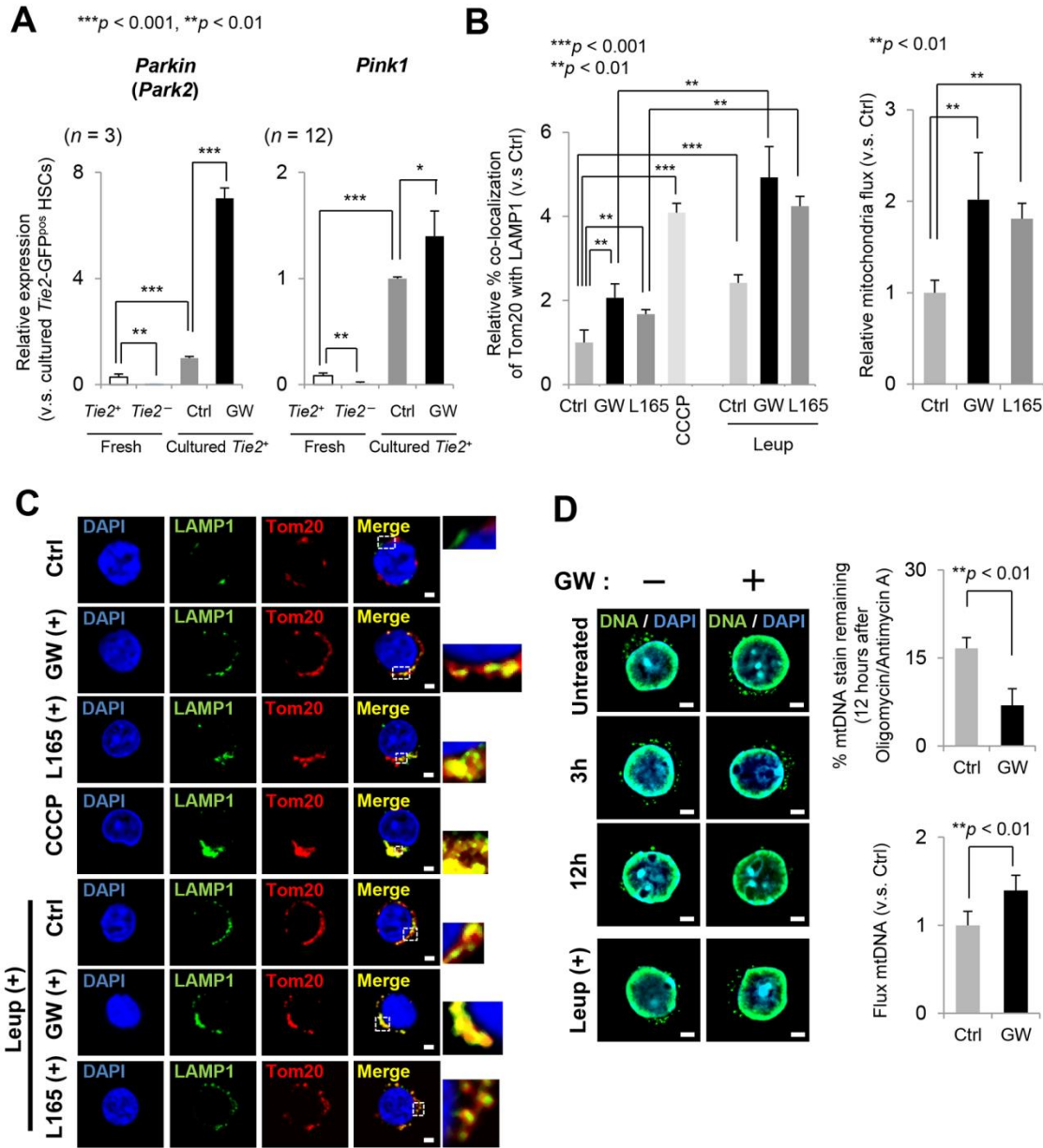


Fig. 2. PPAR-FAO activates mitochondrial autophagy in HSCs. (A) *Parkin* and *Pink1* levels in GW501516-treated (GW) *Tie2*-GFP^{pos} HSCs. (B and C) PPAR δ activators, GW501516 or L-165041 (L165), enhance co-localization of Tom20 with LAMP1. The bars represent mean \pm s.e.m. (at least 10 cells analyzed per each condition per each experiment). CCCP treatment was used as control for mitophagy induction [(B), left]. Mitochondrial net flux calculated by Tom20-accumulation in the presence of leupeptin (Leup) [(B), right]. Representative immunofluorescent (IF) images of co-localized Tom20 with LAMP1 (Tom20, red; LAMP1, green; Merge, yellow) in PPAR δ -agonist-treated HSCs. White dashed boxes represent the magnified images in right. Scale bars, 2 μ m (C). (D) Representative images of GW501516-treated HSCs immune-stained to label mtDNA (left), quantified for mitophagy [12 h oligomycin/antimycin (A)] (right top), and net mtDNA flux (right bottom).

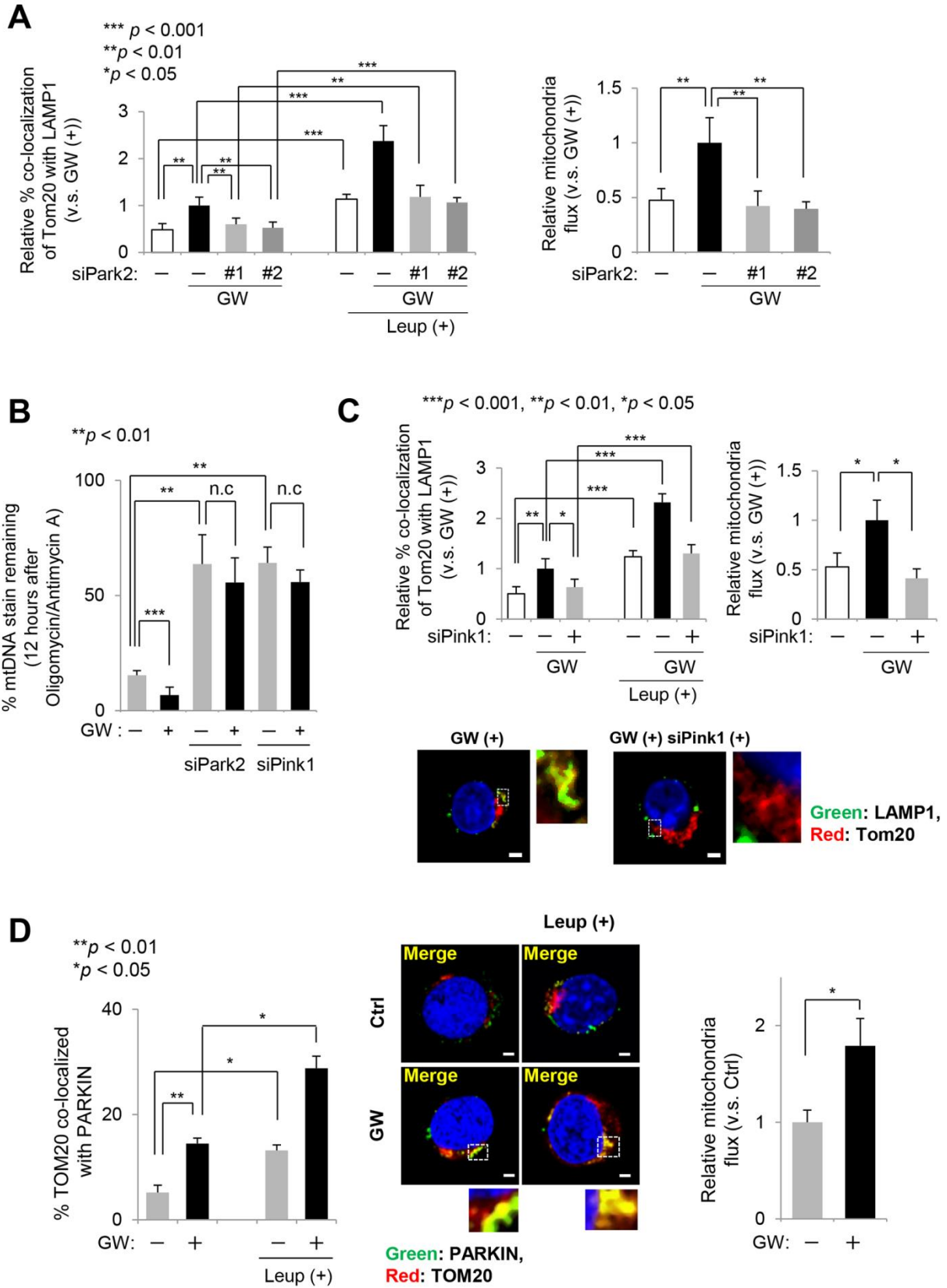


Fig. 3. Parkin is important in PPAR-FAO-induced mitophagy in HSCs. (A) Relative Tom20 co-localization (left) and mitochondria net flux (right) in GW501516-treated HSCs in the presence of siPark2. (B) Quantification of mitophagy based on the remaining mtDNA staining 12 hours after oligomycin/antimycin A treatment. (C) *Pink1*-silencing reduces PPAR δ -enhanced mitophagy. Relative Tom20 co-localization (top left), net mitochondria flux (top right), and representative IF images depicting LAMP1/Tom20 co-localization in GW501516-treated HSCs in the presence of siPink1 (bottom). (D) GW501516 enhances co-localization of TOM20 with PARKIN (left) and mitochondrial net flux (right). Scale bars, 2 μ m.

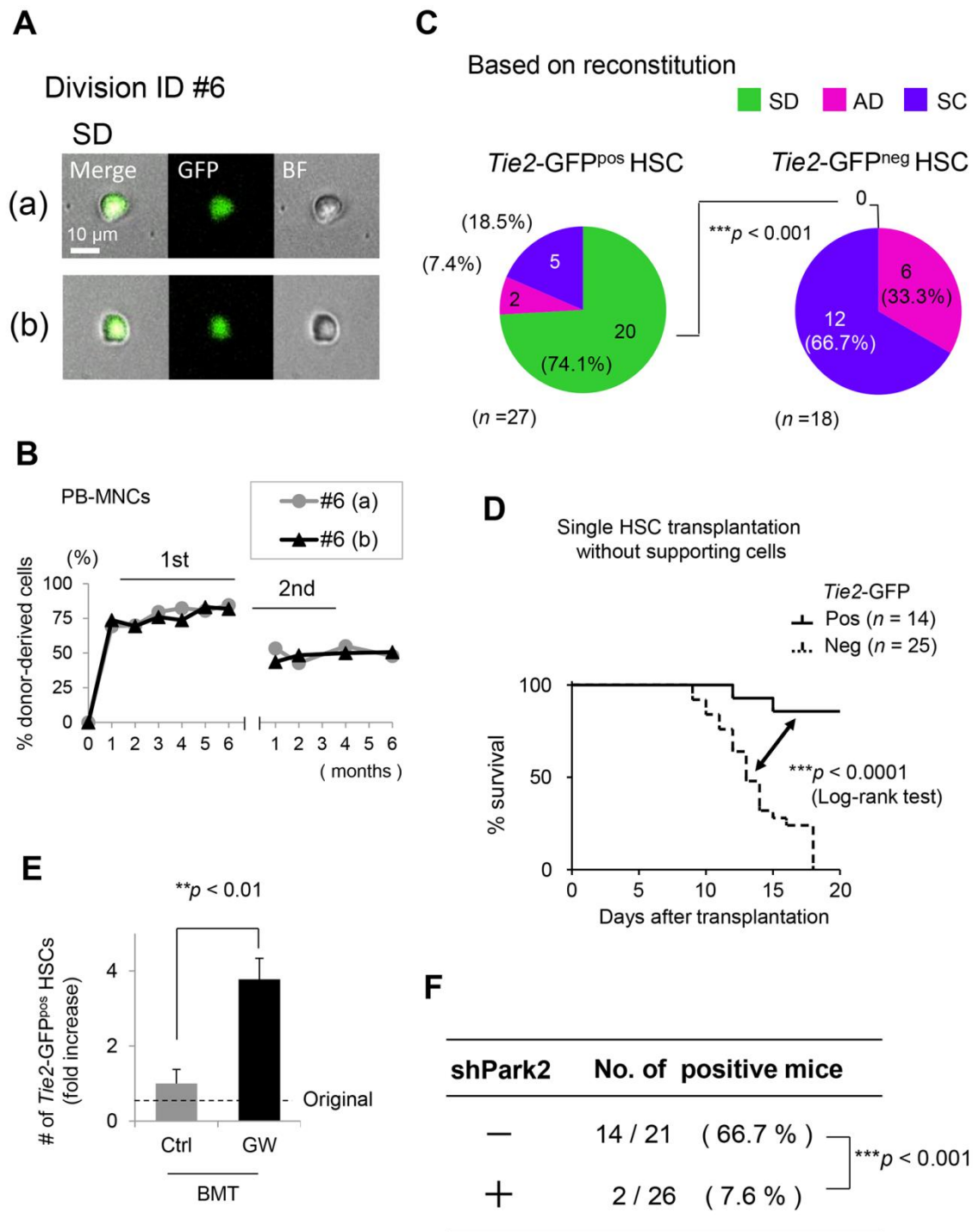


Fig. 4. Self-renewing expansion of *Tie2*^{pos} HSC through mitophagy. (A) Representative pictures of *Tie2*-GFP positivity with bright field (BF) in symmetric division (SD). (B) Representative repopulation kinetics of SD during the 1st and 2nd BMT. (C) Division patterns of *Tie2*-GFP^{pos} HSCs (left) and *Tie2*-GFP^{neg} HSCs (right), in terms of reconstitution capacity. (D) Single *Tie2*-GFP^{pos} HSC transplantation without supporting cells. Survival of recipient mice was examined by Kaplan-Meier survival curves (also see fig. S13B). (E) PPAR δ activation induces *Tie2*-GFP^{pos} HSCs expansion in vivo. The number of transplanted *Tie2*-GFP^{pos} HSCs (donor) is also shown as Original (also see fig. S13H). (F) Frequency of successful hematopoietic reconstitution of shParkin-silenced *Tie2*-GFP^{pos} HSCs (also see fig. S13J).



Self-renewal of a purified *Tie2*⁺ hematopoietic stem cell population relies on mitochondrial clearance

Kyoko Ito, Raphaël Turcotte, Jinhua Cui, Samuel E. Zimmerman, Sandra Pinho, Toshihide Mizoguchi, Fumio Arai, Judith M. Runnels, Clemens Alt, Julie Teruya-Feldstein, Jessica C. Mar, Rajat Singh, Toshio Suda, Charles P. Lin, Paul S. Frenette and Keisuke Ito (October 13, 2016)
published online October 13, 2016

Editor's Summary

This copy is for your personal, non-commercial use only.

- Article Tools** Visit the online version of this article to access the personalization and article tools:
<http://science.sciencemag.org/content/early/2016/10/12/science.aaf5530>
- Permissions** Obtain information about reproducing this article:
<http://www.sciencemag.org/about/permissions.dtl>

Science (print ISSN 0036-8075; online ISSN 1095-9203) is published weekly, except the last week in December, by the American Association for the Advancement of Science, 1200 New York Avenue NW, Washington, DC 20005. Copyright 2016 by the American Association for the Advancement of Science; all rights reserved. The title *Science* is a registered trademark of AAAS.